Journal of Applied Polymer Science

Kinetics and crystallization in pH-sensitive free-radical crosslinking polymerization of acrylic acid

Byungsoo Kim,[1] Daesun Hong,[2] Wenji V. Chang[1]

[1]Mork Family Department of Chemical Engineering and Materials Science, University of Southern California, 925 Bloom Walk, Los Angeles, California 90089

[2]Department of Chemical Engineering, Dankook University, Yongin City, Gyeonggi-Do, Republic of Korea

Correspondence to: W. V. Chang (E-mail: wenji@usc.edu)

ABSTRACT: Free-radical crosslinking polymerization and crystallization of acrylic acid (AAc) were investigated by shear storage modulus (G') measurements in pH 2, as well as in pH 6 and pH 10, by varying the molar ratio of crosslinking agent (*N,N′*-methylene *bis*-acrylamide; MBAAm) to AAc (0.583×10^{-3}, 1.169×10^{-3}, 1.753×10^{-3}, and 2.338×10^{-3}). Our results showed that the pre-gelation time was the same at pH 2, regardless of the concentration of MBAAm. The propagation time was determined by the initial feed concentration of AAc, and the length of the linear curve in the propagation was proportional to the concentration of MBAAm. The Avrami exponent (n), as an indicative of growing pattern of an infinite molecule, in the crystallization was increased in proportional to the concentration of MBAAm, and generally low at pH 2. In the deceleration phase, n was observed near 1.0 throughout the all specimens. These results indicated that (1) the length of the pre-gelation period was determined by the ionization of AAc (or pH), (2) the polymerization rate of AAc was not affected by the concentration of MBAAm, and (3) the inhomogeneity of hydrogel was determined by the growing pattern of infinite molecule in propagation phase. © 2015 Wiley Periodicals, Inc. J. Appl. Polym. Sci. **2015**, *132*, 42195.

KEYWORDS: acrylic acid; crosslinking; crystallization; gels; kinetics

Received 31 December 2014; accepted 13 March 2015

DOI: 10.1002/app.42195

INTRODUCTION

The kinetics of crosslinking polymerization has not been clarified because the addition of a crosslinking agent complicates the reaction mechanism significantly. In addition, problems arising from competing reactions between radicals and multifunctional comonomers,[1] diffusion limitations,[2–4] substitution effects,[5] inhomogeneities in network formation[6] remain unsolved.

Cyclization, which is distinctively observed in a free-radical crosslinking polymerization, leads to the formation of a compact intramolecular cross-linked structure known as microgel,[7] and is due to the reaction between both ends of a growing crosslinking agent molecule. Primary intramolecular cyclization is initiated by one double bond and one radical in a propagating chain, and it would result in a loop structure which does not contribute to the mechanical properties of the hydrogel.[8,9] Primary intramolecular cyclization is independent of the crosslinking agent concentration but is dependent on the total monomer concentration.[10]

Diffusion limitations have been a main concern in free-radical polymerization. Diffusion is more dominant in termination than in propagation. It has been reported that in the event of contact probability, which is decided by the monomer mobility, one reaction may occur per 10^9 collisions during propagation, and one reaction per 10^5 collisions may occur during termination.[11] The k_p/k_t (propagation kinetic constant/termination kinetic constant) ratio was near 10^{-3} in the copolymerization of acrylamide (AAm) and MBAAm,[12] and 10^{-3} to 10^{-5} until 50%–60% conversion in the copolymerization of styrene and divinyl benzene.[13,14] Propagation progresses by the reaction of one large radical and small monomer molecules, and thus, is much less hindered by diffusion.[13]

Bimolecular termination occurs by a consecutive three-step reaction: two radical coils approach each other by translational diffusion (center of mass diffusion of the active polymer chains); segmental diffusion reorients the polymer molecules until their chain ends come in close contact with each other; and the chain ends react chemically via the so-called reaction diffusion (activation energy required for the two radical ends to react).[15,16] At low conversions, the small polymer coils easily achieve translational mobility, and segmental diffusion becomes the rate-determining step in termination.[17–20]

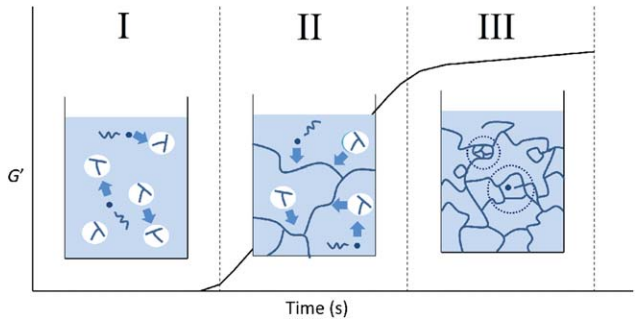

Figure 1. Free-radical crosslinking polymerization of AAc was achieved by three steps—pre-gelation (phase 1), propagation (phase 2), and deceleration (phase 3). Infinite molecule was formed with the growth of branched molecules, increased G'. [Color figure can be viewed in the online issue, which is available at wileyonlinelibrary.com.]

However, at high conversions, reaction diffusion is dominant, while segmental and translational diffusions are neglected because of the immobility of the chain.[21]

One of the main differences between linear polymerization and crosslinking polymerization is that the conversion rate, which affects the type of dominant diffusion for termination, is lower in the latter. Reaction diffusion-controlled termination is seen after 40%–50% conversion in the case of linear polymerization; in cross-linking polymerization, this type of termination is seen after 5% conversion, and it dominates after 15% conversion, where k_p/k_t becomes constant.[13,22–24]

Network inhomogeneity throughout the polymerization is another problem to be solved to improve its mechanical property and to obtain more consistent results.[25–30] In case of the living radical linear polymerization to decrease M_n/M_w [polydispersity index (PDI)], kinetic chain propagation ceases when all the monomers are consumed, because there is no termination step.[31,32] However, in crosslinking polymerization, this pattern would not be too effective to afford a homogeneous structure. It was reported that the iniferter (initiator–transfer agent–terminator) was not so effective to improve the homogeneity of hydrogel.[31]

Thus, for three main issues—primary intramolecular cyclization, termination, and inhomogeneity in free-radical crosslinking polymerization, we set the concentration of AAc constant in all measurements to minimize the effect of primary intramolecular cyclization on the polymerization, divided reaction time into three intervals (Figure 1) and monitored the increase of G' when the termination by reaction diffusion was dominant, and compared n in the Avrami equation with $G'(t)/G'_{max}$ values to investigate inhomogeneity throughout the polymerization, varying pH value and the concentration of MBAAm.

From our real-time G' measurement as a direct output of network formation, it was expected to elucidate the relationship between the polymerization rate of AAc and the concentration of MBAAm, and the effects of pH on the pre-gelation period and the inhomogeneity. At the deceleration phase, n was not much different to each condition due to monomer composition drift or radical inefficiency.[33]

EXPERIMENTAL

Materials

AAc (anhydrous 99%) was purchased from Aldrich Chemical. MBAAm was purchased from Fluka. Ammonium persulfate (APS) (98+%, A.C.S. reagent) was purchased from Sigma-Aldrich. Potassium phosphate monobasic and sodium hydroxide were purchased from Mallinckrodt. Hydrochloric acid (Reagent A.C.S.) was purchased from Fisher Scientific. All these chemicals were used as received.

Preparation of Solutions with the Desired pH

Two solutions with different pH levels were prepared to examine the effect of pH on the gelation behavior. Solutions (nonbuffers) of pH 2 and 10 were prepared by mixing appropriate volumes of diluted HCl (pH 2, 0.1*M*) and NaOH (pH 13, 0.1*M*) stock solutions. The pH value of the DI water used as a reaction medium was about 6.0. With pH meter, it took about 20 h for the pH value to be stabilized because ions were rare in the solution.

Crosslinking Polymerization

Hydrogels were prepared by free-radical crosslinking polymerization. The initial solution consisted of AAc, MBAAm, and pH solutions. As shown in Table I, the MBAAm/monomer molar ratios were 0.583×10^{-3}, 1.169×10^{-3}, 1.753×10^{-3}, and 2.338×10^{-3}. The solid content was fixed to 23 wt % to reduce the termination reaction during the gelation. Before corresponding chemicals were poured into the reactor, which had a double-gap cylindrical geometry (DG27, MCR 301, Physica, Anton Paar), the solution was stirred and deoxygenated by bubbling with nitrogen gas for 20 min. When the solution temperature reached to 60°C, the initiator APS solution was added, and allowed the reaction to proceed to completion. The polymerization time was 60 min for all samples.

Measurement of G′

Measurements of G' were performed in the time sweep mode. The gap between the cylinder and the bottom of the reactor was kept at 2 mm. The shear strain (amplitude gamma) was 1%, and the frequency was 1 Hz. The temperature, which was fixed at 60°C, was controlled by a water bath controller (Julobo, F25). The amount of initial gel solution poured into DG27 was 7 mL. After temperature reached 60°C, 1 mL of initiator solution was added. The time gap between the addition of the initiator solution and the starting time of the measurements was 15 s. A total of 30 points were scanned with a time interval of 2 min between each point.

RESULTS AND DISCUSSION

The goal of this study is to investigate the effects of pH and the concentration of MBAAm on crosslinking polymerization of AAc, as previously mentioned. We tried to interpret more in detail the crosslinking polymerization of acrylic acid in view of time intervals of each phase, slope of each curve, and inhomogeneity for a course of polymerization, which were not managed in our previous work—G' and tanδ were monitored and compared in the crosslinking polymerizations of three acrylic monomers.[34] Thus, first, we investigated the condition for network formation. Second, the increase and slope of G' were monitored

Table I. Chemicals Used for Crosslinking Polymerizations of AAc

Code[a]	MBAAm (mg)	AAc (mL)[b]	APS (mg)	pH solution (mL)[c]	([MBAAm]/[AAc]) × 10^3
AAc1	2.83	2.16	13.44	8.0	0.583
AAc2	5.66	2.16	13.44	8.0	1.169
AAc3	8.49	2.16	13.44	8.0	1.753
AAc4	11.32	2.16	13.44	8.0	2.338

[a] [MBAAm]: mol of MBAAm, [AAc]: mol of AAc.
[b] Density of AAc is 1.05 g/mL.
[c] Solid wt % is 23% [(wt of monomer)/(wt of monomer + wt of pH solution)].

at phase 2 and 3. Last, n was plotted from Avrami equation with $G'(t)/G'_{max}$ values of relevance to the inhomogeneous growth of infinite molecule. The criteria to determine the end of phase 1 was the increase of G' with the formation of infinite molecule. End of phase 2 was determined when the curve became leveled off after the inflection point. At this range where phases 2 and 3 coexisted, it was believed that (1) most branched molecules were already attached on the infinite molecule or entrapped, and (2) AAc molecules dissolved in solution were reacted with network or entrapped molecules. Propagation and incorporation of branched molecules to the infinite molecule, and network growth by AAc were assumed to induce the steep increase of G' during phase 2.

Condition for Network formation

The primary condition for network formation is the growth of an infinitely large molecule in three dimensions.[35] To achieve this structure, two preliminary conditions should be met: (1) generation of trifunctional molecules or multifunctional molecules and (2) a higher probability of propagation than termination.

In linear polymerization, chain propagation proceeds in one direction because only one radical is present in a chain. If a chain which is not linear has two functionalities (radical or vinyl group), a branched structure would be formed. In crosslinking polymerization, trifunctional molecules act as junctions and produce a network structure [Figure 2(a)]. These trifunctional molecules can be generated by the reaction between two pendant double bonds (PDB).

In Figure 2(b), which presents eight possible reactions between PDBs–between radicals or radical and double-bonds, the probability of formation of trifunctional molecules is about 50% (4 trifunctional molecules produced from 16 PDBs), and the probability of formation of dead molecules is 12.5%. About 37.5% of these reactions afforded bifunctional molecules. We did not consider the further reactions between trifunctional or bifunctional molecules, which were generated from PDB reactions; rather, we hypothesized that the inefficiency of the trifunctional molecules would offset the probability of regenerating trifunctional molecules.

As the second criterion for network formation, Flory[36] reported that the minimum number of the radicals in the branch units should propagate; otherwise, the molecule would be a dead polymer. This least probability (α) is dependent on the number of functionalities (f): $\alpha = 1/(f-1)$; for example, if f is 5, α would be 25%. Thus, at least 2 of 5 radicals should not be terminated. The minimum number of end radicals (N_{min}) that should be involved in the propagation increases with the generation number. If trifunctional molecules are attached to each end of chain, the number of branches in the second generation would be 6 (while the number of branches in the first generation is 3). In this case, more than three radicals at the ends of the branched unit must propagate. Thus, N_{min} would be expressed by

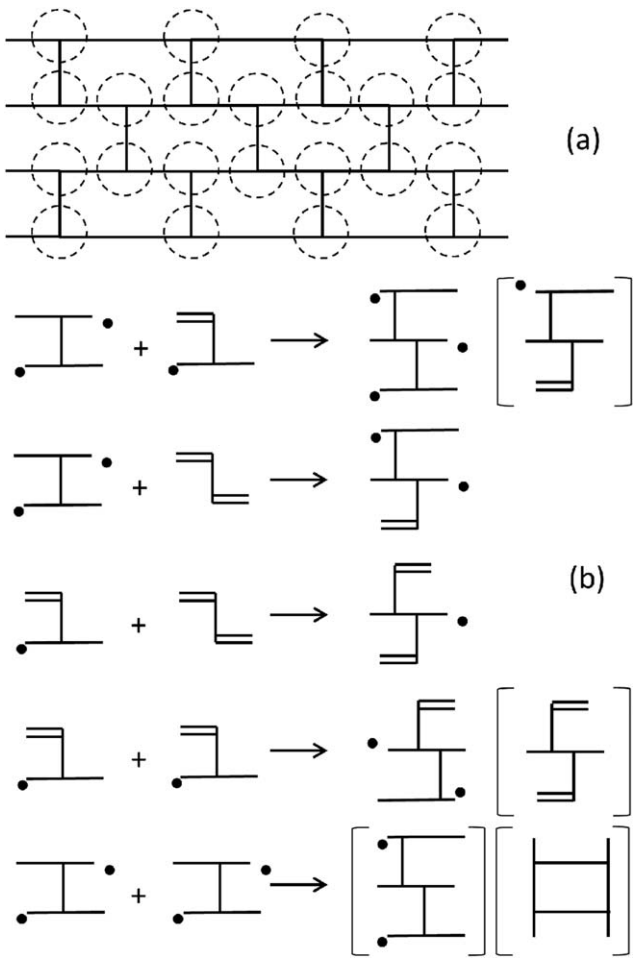

Figure 2. (**a**) Network could be formed by the reaction between trifunctional molecules, (**b**) Possible reactions between pendant double bonds (PDB) to generate trifunctional molecules

$$N_{\min} = \left(\frac{f}{f-1}\right) \times 2^{g-1} \quad (1)$$

where g is the number of generation.

The issue that is not considered in eq. (1) is the uncertainty in the number of nucleation molecules (1st generation) which is related to the concentrations of initiator and crosslinking agent, mainly produced in the pre-gelation period and the probability of formation of the infinite molecule even if $N_{\min}$ decreases with an increase in the generation number, provided the close distance or the short time gap between each nucleation to facilitate the bridge formation.

Thus, we first considered the average molecular weight between crosslinks (M_c), so called "mesh size." M_c, which is a nominal value conventionally known to be 0.5 × ([AAc]/[MBAAm]) was modified as follows:

$$M_c = \frac{2}{3} \times \frac{X_c[\mathrm{AAc}]}{0.25[\mathrm{MBAAm}]} \quad (2)$$

where [AAc] and [MBAAm] are the initial feed concentrations (mol) of AAc and MBAAm, respectively, and 0.25 × [MBAAm] means the fraction of trifunctional molecules generated in the initial concentration of MBAAm. X_c is the conversion rate of the monomer. In Table I, [AAc] is 0.0315, and [MBAAm] is 1.838×10^{-5}, 3.675×10^{-5}, 5.513×10^{-5}, and 7.351×10^{-5}, respectively. X_c at the end of phase 2 was about 90%. Thus, M_c (g/mol) was 4114, 2057, 1371, and 1028 for each corresponding MBAAm concentration.

Malkin *et al.*[37] reported that the number-average degree of polymerization ($\bar{N}$) in free-radical linear polymerization could be expressed as

$$\bar{N} = \frac{X_c[\mathrm{AAc}]}{[I]_0 - [I]} \quad (3)$$

where $[I]_0$ is the initial feed concentration of the initiator and $[I]$ is the current concentration of the initiator. The term $[I]_0 - [I]$ denotes the decomposed concentration of the initiator. Therefore, the average number of junctions (N_{CR}) per branched molecule as a function of initiator concentration is equal to the term of $\bar{N}$ [eq. (3)] divided by M_c [eq. (2)], and expressed as follows,

$$N_{CR} = \frac{0.375[\mathrm{MBAAm}]}{[I]_0 - [I]} \quad (4)$$

In trifunctional crosslinking, the number of junctions is given by $3 \times (2^{g-1}) = N_{CR} + 2$. Thus, if eq. (4) can be rewritten as $(2^{g-1}) = (1/3)\ [(0.375\{\mathrm{MBAAm}\}/\{[I]\text{-}[I]_0\}) + 2]$, and if this equation is substituted in eq. (1), the average minimum number of radicals required to form the network per branched molecule will be expressed as a function of [MBAAm] and ($[I]_0 - [I]$).

$$N_{\min} = \frac{1}{2}\left(\frac{0.375[\mathrm{MBAAm}]}{[I]_0 - [I]} + 2\right) \quad (5)$$

Therefore, the minimum condition to form the network could be found in eqs. (1) and (5). For example, in case of trifunctional molecules (1st generation), $N_{\min}$ is 1.5 in eq. (1). If this is substituted into eq. (5), $[\mathrm{MBAAm}]/([I] - [I]_0]$ should be lower than 2.66. In Table I, the molar ratio of [MBAAm]/[APS] is 0.31–1.24, which satisfies the minimum condition of network formation. However, this hypothesis does not include two variables—(1) fraction of primary intramolecular cyclization that decreases the efficiency of crosslinking, which related to the total monomer concentration, and (2) the efficiency of initiator. Values of 0.31–1.24 were obtained with the assumption that the fraction of primary intramolecular cyclization was zero, and the efficiency of initiator was 100%. It will be considered with further studies to find more exact values in the future.

Efficiency of PDB in Phase 1: Effects of Concentration of Crosslinking Agent and pH

Several reactions in crosslinking polymerization make the crosslinking agent inefficient: primary or secondary cyclization, intermolecular, and intramolecular terminations. These reactions result in looping, dangling, and dead polymers. Dangling chains are an elastically inactive part of the network structure, which do not contribute to stress.[38] Loose, dangling chain ends attached to the network by only one end are regarded as defects that tend to decrease the retractive stress.[39–41] Tobita and Hamielec[42] reported that 80% of the PDBs are consumed by primary cyclization reactions when the overall weight fraction of AAm and MBAAm is 5.6%. Secondary cyclization was about 1000 times more effective in consuming PDBs than was crosslinking. Okay *et al.*[43] estimated that 95% of the PDBs underwent primary cyclization if the solid weight fraction was 5%. The primary cyclization is influenced by chain flexibility, primary chain length, and solvent quality, apart from the weight fraction of the monomer.[10]

However, the extent of cyclization of PDBs in crosslinking polymerization would be mostly dependent on the type of monomer and PDB, as well as the conversion rate of the monomer. The extent of cyclization involving PDBs consuming was 80% in the AAm/MBAAm system and 30% in the methyl methacrylate (MMA)/ethylene glycol dimethacrylate (EGDM) system at zero conversion.[42–45]

Fast polymerization of AAc and low reactivity of PDBs could increase the time gap among the reactions between the first and the second functionalities of PDB. This would reduce the probability of cyclization because the gap between the propagating chain lengths of the first functionalities and second functionalities of a PDB would be large. However, this hypothesis is trivial or ineffective in improving the efficiency of PDBs. The reactivity of a PDB is dependent on the distance between two PDB radicals, but is independent of the propagation rate; this is because the termination reaction is orders of magnitude faster than the propagation reaction, which induces diffusion-based polymerization.[31]

Based on the above facts, at the pre-gelation period, it is evident the polymerization rate does not significantly affect the efficiency of PDB; in other words, monomer concentration is not a key parameter to improve the homogeneity of the hydrogel if it is not significantly different. Instead, ionization of the monomer or other conditions to control the distance between radicals and monomers would be more important for the efficiency of PDBs.

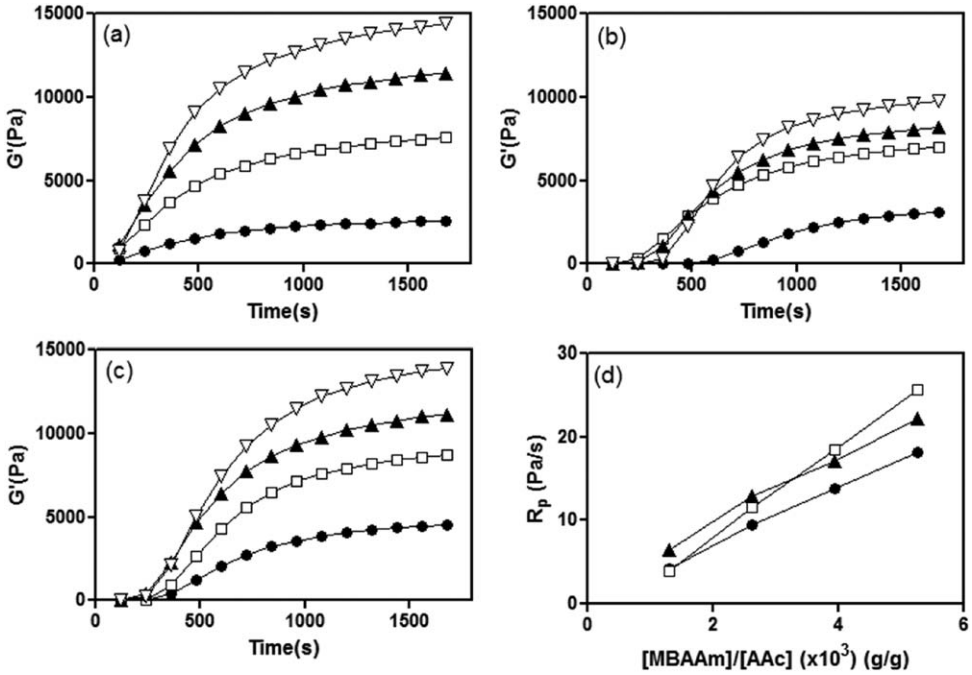

Figure 3. G'(Pa) behaviors to the crosslinking polymerization of AAc in phases of pre-gelation and propagation, (-•-) AAc1, (-□-) AAc2, (-▲-) AAc3, and (-▽-) AAc4, (**a**) at pH 2, (**b**) at pH 6, (**c**) at pH 10, and (**d**) rate of network formation as a function of pH and the concentration of MBAAm, (-■-) at pH 2, (-○-) at pH 6, and (-△-) at pH 10. R_p denotes the rate of network formation.

Propagation Rate of an Infinite Molecule in Phase 2: Effects of Concentration of Crosslinking Agent and pH

In this study, free-radical crosslinking polymerization was conducted at different pH levels. The ionization of AAc was expected to affect the termination rate or efficiency of PDB based on the chain mobility and the distance between radicals. The rates of network formation at different pH levels were monitored by measurements of G'. Termination would be limited by the immobility of chains in phase 2.

G' increased with the formation of an infinite molecule, and the slope of each curve was influenced by the concentration of MBAAm. G' behaviors in phases 1 and 2 are presented in Figure 3. All the curves were stabilized at about 30 min, by the end of phase 2. At this point, G' (Pa) ranged from 2580 to 14,400 at pH 2 [Figure 3(a)], from 3116 to 9780 in the case of pH 6 [Figure 3(b)], and from 4540 to 13,900 at pH 10 [Figure 3(c)].

The pre-gelation period was not significantly influenced by the concentration of the crosslinking agent, but was influenced by the pH. The range of this time period ends after 70–80 s at pH 2, 180–360 s in pH 6, and 120–180 s at pH 10. The feed concentration of the crosslinking agent was up to four-fold different, but the gap between the lowest and highest time points were much narrower.

The slopes before the inflection points of each curve are compared in Figure 3(d). The increase in the slope with the concentration of crosslinking agent was consistent for pH 6 and at pH 10, but steeper at pH 2.

The polymerization rate of AAc was independent of the MBAAm concentration. First, in the propagation phase, the time period was determined by the initial feed concentration of AAc, and the length of the curve was influenced by the MBAAm concentration. The inflection points were observed near 750 s for pH 6 [Figure 3(b)] and pH 10 [Figure 3(c)], and at 600 s for pH 2 [Figure 3(a)]. However, the augment points (end of pre-gelation) at pH 2 appeared about 150 s earlier than that for pH 6 and pH 10. Thus, the time lag between the augment and inflection points was similar for all pH ranges.

Second, the slope linearly increased with the MBAAm concentration. $G'(t)/G'_{max}$ curves for pH 6, pH 2, and pH 10 are plotted in Figure 4. The increasing ratio of $G'(t)$ to G'_{max} was the

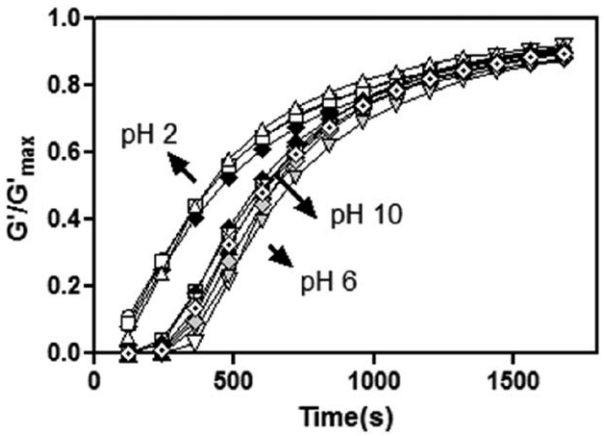

Figure 4. G'/G'_{max} behaviors—curves for four concentrations of MBAAm were converged to one master curve at each pH. G'/G'_{max} was increased faster in the order pH 2 > pH 10 > pH 6.

same, regardless of the MBAAm concentration: four curves converged into one master curve. Thus, three master curves were plotted against pH. The relationship between the efficiency and concentration of PDBs may be dependent on the intrinsic property or the ionization of monomer.

Lattuada *et al.*[46] reported Monte Carlo simulations of the crosslinking polymerizations of MMA and AAm. In their simulation, the termination rate was low and the polymerization rate was high because of the high amount of radicals produced when the amount of crosslinking agent was increased. Batch *et al.*[33] reported kinetic models of the crosslinking polymerization of divinyl benzene and vinyl ester. In their study, a higher fraction of crosslinking agent induced a lower polymerization rate. The following explanation was provided: unimolecular radical trapping was promoted when increasing the concentration of crosslinking agent, even if the crosslinking agent decreased the rate of bimolecular termination.

Keskinel and Okay[7] compared MMA/EGDM and AAm/MBAAm systems on the basis of the polymerization rate of the monomer. In the MMA/EGDM system, the polymerization rate did not differ drastically with the concentration of EGDM (the difference in conversion rate was below 3% after 3 h), and in the AAm/MBAAm system, the polymerization rate increased when sodium acrylate (NaAc) or 2-acrylamide-2-methylpropanesulfonic acid sodium salt (NaAMPS) was added as a comonomer. Further, the termination rate of ionic macro-radicals was lower than that of non-ionic radicals at high concentrations of the crosslinking agent.

The efficiency of MBAAm in AAc crosslinking polymerization was different at pH 2. The p*K*a of AAc is known to be about 5.0.[34] Thus, at pH 2, most of the carboxyl groups of AAc were not ionized, which resulted in a shorter distance between AAc molecules and radicals in solution as compared with that for pH 6 and pH 10. When a PDB reacts with propagating radical chains, there is an increased probability of the radical on the PDB coming in contact with the nearby monomer. This in turn may increase the efficiency of PDBs (decreasing the number of intramolecular cyclizations). As seen in Figure 3(d), the efficiency of PDBs was influenced to a greater extent by the concentration of PDBs than at pH 6 and pH 10, owing to the lack of ionization. However, at pH 10, the efficiency of PDBs was higher than at pH 6 because of the greater mobility induced by the stronger electrostatic repulsion force.

Therefore, in our system, the polymerization rate of AAc was independent of MBAAm concentration, and the reactivity of MBAAm toward AAc radicals increased with the ionization of AAc because of the increased mobility even if the distance between MBAAm and AAc radicals was similar at pH 6 and pH 10. The dependence of the reactivity of MBAAm toward AAc radicals on the MBAAm concentration was higher at pH 2. The augment time of phase 2 with increase of G' at pH 2 was faster than at pH 6 and pH 10, and it was due to the shorter distance between AAc and PDB radicals increased the dependency of the reactivity of PDBs on the PDB concentration. Thus, the reactivity of MBAAm would be high in the order of at pH 2 > pH 10 > pH 6.

Termination could be significantly reduced after the infinite molecule was formed at the beginning of phase 2. Diffusion-limited bimolecular termination was more hindered after the radicals were attached to the network, and termination might be insignificant.[33] The decreased termination rate in this phase would be caused by an increase in the viscosity of the system and the mechanism of reaction diffusion termination, that is, the termination of diffusion-limited immobile chain radicals formed by growth through the propagation.[47,48] Several studies[49–51] also reported that the termination coefficient became constant to the double-bond conversion as it was proportional to the propagation kinetic constant, where reaction diffusion was the primary mode of termination. Intramolecular terminations (between two functional groups on the same molecule) could be neglected, based on Kienle *et al.*'s study on glycerol-dibasic acid.[52] Bradley's report[53] on drying oil resins stated that the number of consumed molecules was slightly less than the number of inter-unit linkages formed. Therefore, it could be possible to exclude the termination in this phase.

Herein, the network formation was reinterpreted by the crystallization behavior. Crystallization progresses via nucleation and crystal growth. During nucleation, branched molecules converge to the infinite molecule via chain propagation or intermolecular reaction. This type of nucleation is categorized as contact nucleation.[54]

The kinetics of network formation at pH 2, pH 6, and pH 10 in Figure 5, as evaluated from $G'(t)/G'_{max}$ measurements, were analyzed using the Avrami equation,[55,56]

$$1-\frac{G'(t)}{G'_{max}}=\exp(-kt^n) \quad (6)$$

G'_{max} is the value of G' after 1 h of polymerization, and the ratio $G'(t)/G'_{max}$ represents the extent of gelation. The Avrami equation using the value of $G'(t)/G'_{max}$ allows us to find the exponent n that governs the crystallization kinetics. The values of G'_{max} are listed in Table II. n values obtained from the linear fit at pH 2 [Figure 5(a)], pH 6 [Figure 5(b)], and pH 10 [Figure 5(c)] were 1.5–2.3, 2.8–5.7, and 3.0–3.6, respectively. It is worth noting that the maximum variation in $G'(t)/G'_{max}$ does not exceed 2% even if G'_{max} is obtained at 2 h of polymerization, because the increasing slopes of G' in phase 3 are below 0.6 (Pa/s) [Figure 6(b)]. This means that the determination of G'_{max} after 1 h of polymerization is relatively insensitive to the kinetics.

In Figure 5, about four points were taken out of Figure 4. As explained previously, the infinite molecule is propagated by the incorporation of branched molecules and AAc. In the transition region between phase 2 and phase 3, it was thought that most branched molecules already incorporated (except entrapped ones), and the infinite molecule propagated only by AAc. With depletion of AAc in solution, phase 3 started. Thus, we have tried to get n values which are for the network growth by both branched molecules and AAc, not only by AAc, and excluded that coexisted region.

There is no clear interpretation of n, but it is generally known that n ranges between 1 and 4.[57] Crystallization is progressed

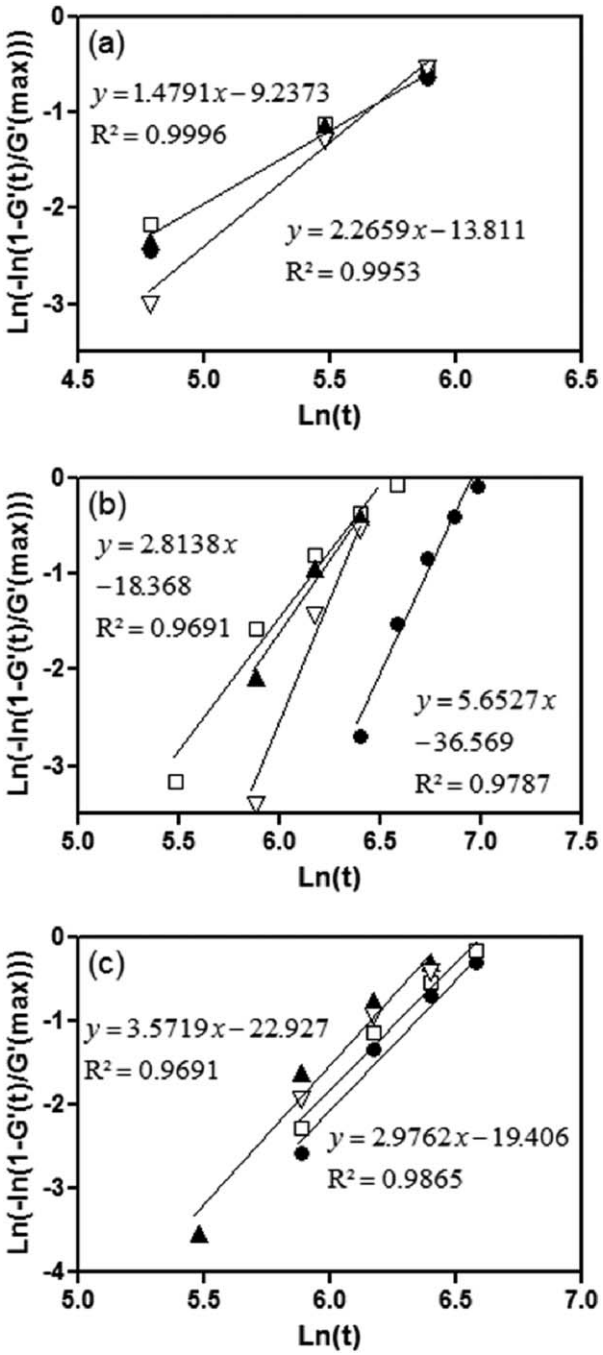

Figure 5. Linear fittings of Avrami equation in phase two. Avrami exponent (n) was found from the slope of each curve. (-•-) AAc1, (-□-) AAc2, (-▲-) AAc3, and (-▽-) AAc4, (**a**) at pH 2, (**b**) at pH 6, and (**c**) at pH 10.

on the surface if n is about 1, and inside if n is over 3. An n value of more than 3 implies three-dimensional growth,[58] which is usually observed at the beginning of the nucleation.[57] In our result, the highest value of n was observed for AAc4 at pH 6, 5.7, and the gap between the lowest and highest was the most significant at pH 6, 2.8–5.7. The n value was in the order pH 6 > pH 10 > pH 2. Further, n increased in proportional to the concentration of MBAAm.

The n value indicates the change in the nucleation pattern. A more random growth would result in higher values of n, exceeding 3. In other words, as more MBAAm is incorporated, the number of growth directions would increase. This behavior is regardless of the number of chain radicals because the initial feed concentration of the initiator is the same for all specimens and the termination reaction in this phase is not significant.

Thus, the above behavior could be explained by two aspects. First, as n is higher, there is a higher concentration of defects such as looping, dangling, or dead polymers, which proportionally increase with the concentration of MBAAm, and induce a greater number of growing directions when encountered. Thus, based on our results, the efficiency of PDBs is the highest at pH 2, and the G' values of AAc3 and AAc4 at pH 6 are much lower than those at pH 2 and 10 (Figure 3); PDB was generally more efficient as n was lower, given the same concentration of MBAAm.

Second, based on the fact that n was higher at high MBAAm concentration, n increased with a decrease in the size of clusters that were separated from the infinite molecule. It has been reported that the local concentration of PDBs within a cluster separated from the infinite molecule should increase as the concentration of MBAAm increased.[7] Each cluster would tend to form more cycles and result in a more compact structure. As the size of cluster decreases, the probability of growth of the infinite molecule inside its structure would be higher.

At pH 2, n is generally low, and this means that the size of each cluster is large. This might imply that nucleation was progressed on the surface of the infinite molecule. Therefore, it could be inferred that the structure was more homogeneous as the size of the cluster separated from the infinite molecule was larger. This behavior could be traced by the value of n.

Rate of Microgel Formation in Phase 3: Effects of Concentration of Crosslinking Agent and pH

In phase 3—the deceleration phase—which was observed after 30 min of polymerization, the rate of network formation was severely reduced. In general, from 30 to 60 min of polymerization, about 10% increase in G' was observed. The conversion rate was about 90% at 30 min [Figure 6(a)].

The reduced polymerization rate in this phase could be possibly ascribed to the exhausted AAc molecules in solution. If AAc molecules exist in solution, chain propagation of network is still possible because AAc is one order-of-magnitude smaller than mesh size, and water-soluble, thus its mobility is not limited by the network.

Table II. Maximum Values of G' at pH 2, pH 6, and pH 10

G'_{max} (Pa)	pH 2	pH 6	pH 10
AAc1	2,930	3,674	5,170
AAc2	8,350	7,846	9,690
AAc3	12,700	9,004	12,300
AAc4	15,600	10,690	15,500

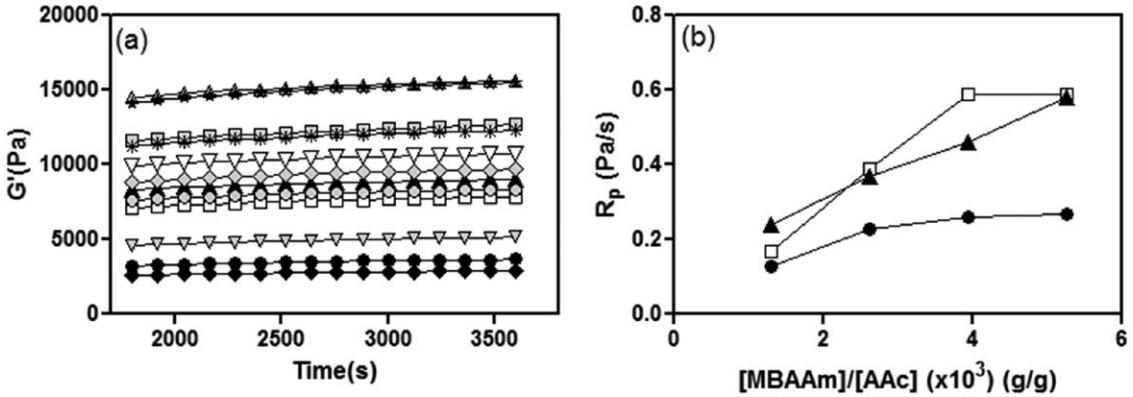

Figure 6. (**a**) G'(Pa) behaviors to the crosslinking polymerization of AAc in the phase of deceleration, (-◆-) AAc1 at pH 2, (- --) AAc2 at pH 2, (- -) AAc3 at pH 2, (- -) AAc4 at pH 2, (-•-) AAc1 at pH 6, (-□-) AAc2 at pH 6, (-▲-) AAc3 at pH 6, (-▽-) AAc4 at pH 6, (- -) AAc1 at pH 10, (- -) AAc2 at pH 10, (-Ж-) AAc3 at pH 10, and (-★-) at AAc4 at pH 10, and (**b**) rate of network formation as a function of pH and the concentration of MBAAm, (-■-) at pH 2, (-○-) at pH 6, and (-△-) at pH 10. R_p denotes the rate of network formation.

Thus, it could be assumed that the trapped radicals from the network chain could not come in contact with the AAc molecules, but rather came in contact with the other radicals and induced termination (even if this probability was low), or encountered trapped PDBs. Kloosterboer *et al.*[59] reported that many PDB molecules could be entrapped in the microgel regions, which decreased the reactivity of PDBs because of steric hindrance. Ward and Peppas[31] reported that the homogeneity could be controlled by the reactivity of PDBs, and not by the polymerization rate. Besides these reports, in our all specimens, this independence of microgel formation on the polymerization rate could be also explained by the similar increase (10%) in G'. The entrapped growing PDBs may show similar probabilities of interacting with radicals in other PDBs or in the network chain.

As shown in Figure 6(b), the increase in G' was higher as the concentration of MBAAm was increased. This behavior was generally similar to that in phase 2 [Figure 3(d)]. The slope increased most steeply at pH 2, and the gap in the curves at pH 6 and pH 10 was almost constant. Thus, it was hypothesized that network growth still progressed, although at a low rate.

Figure 7 presents the growth rate of the network in phase 3. The n value at pH 2, pH 6, and pH 10 was in the range of 1.0 to 1.4 (Figure 8(a–c)]. The interesting point to be noted is that n is generally independent on the pH value and the concentration of MBAAm.

The non-linear regions at the end of curves in Figure 8 have been considered in R^2. These non-linear regions were ascribed to the slower decrease of values of $1 - G'(t)/G'_{max}$ since $G'(t)/G'_{max}$ increased more slowly as it approached to 1.0 in that corresponding region. This induced the faster increase of $\ln[-\ln(1 - G'(t)/G'_{max})]$. It could be interpreted to the reduced rate of reaction between functionalities of network.

CONCLUSIONS

G' was measured to monitor the effects of ionization and the concentration of MBAAm on the rate of network formation at pH 2, pH 6, and pH 10. The crystallization behaviors in the propagation phase and deceleration phase were determined from the plots of $G'(t)/G'_{max}$ and n values from the Avrami equation.

The condition for network formation was dependent on the ratio of MBAAm concentration and the radical concentration, if the concentration of AAc was not significantly different. Numbers of junctions per branched unit could be related to the structure of hydrogel. However, in this crosslinking polymerization of AAc as an ionic monomer, ionization of AAc and pH of solution were more important factors to determine the period of pre-gelation than the polymerization rate. This might be induced from the fact that the efficiency of PDB was dependent on the ionization of AAc.

In the propagation phase, G' showed a steep increase. The polymerization rate of AAc was independent of the concentration of MBAAm and ionization, because the length of this period was the same for all specimens, and the $G'(t)/G'_{max}$ curve was the same at four different concentrations of MBAAm but differed with pH. Crystallization in this phase indicated nucleation—

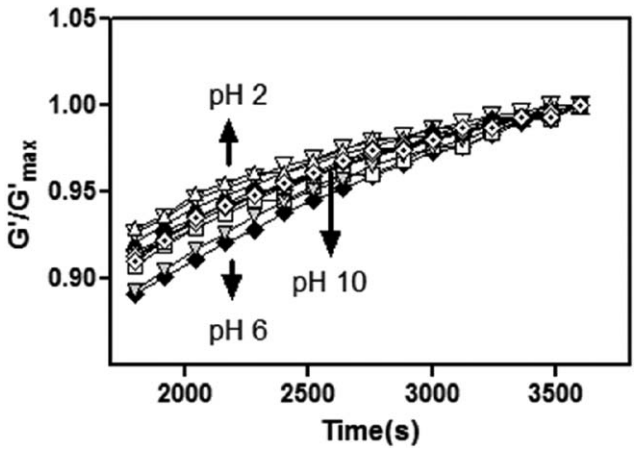

Figure 7. G'/G'_{max} behaviors in the deceleration phase—curves for four concentrations of MBAAm were converged to one master curve at each pH.

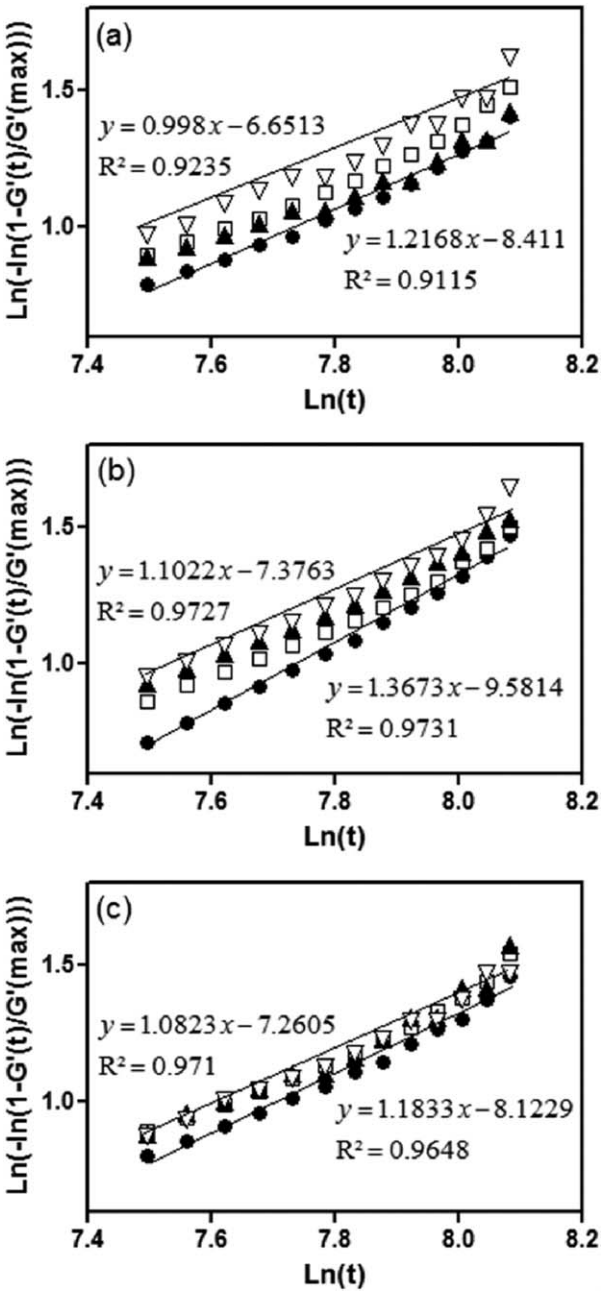

Figure 8. Linear fittings of Avrami equation in phase three. *n* was found from the slope of each curve. (-•-) AAc1, (-□-) AAc2, (-▲-) AAc3, and (-▽-) AAc4, (**a**) at pH 2, (**b**) at pH 6, and (**c**) at pH 10.

growth of the infinite molecule; branched molecules separated from the infinite molecule were more compact as the concentration of MBAAm was increased. The low values of *n* at pH 2 were attributed to the fact that the infinite molecule propagated faster with the larger branched molecules on its surface.

The termination reactions in phases 2 and 3 were not significant because of the immobility of chain. The number of junctions in each branched unit was not much affected by the concentration of AAc, even if the mesh size was influenced by the concentration of AAc. Moreover, in phases 2 (sufficient monomers) and 3 (exhausted monomers), the efficiency of PDBs and its dependency on the PDB concentration were similar and were determined by the ionization, that is, different pH levels.

REFERENCES

1. Stevenson, J. F. *Polym. Eng. Sci.* **1986**, *26*, 746.
2. Huang, Y. J.; Lee, L. J. *AIChE J.* **1985**, *31*, 1585.
3. Atherton, J. N.; North, A. M. *Trans. Faraday Soc.* **1962**, *58*, 2049.
4. Walling, C. *J. Am. Chem. Soc.* **1949**, *71*, 1930.
5. Fink, J. K. *J. Polym. Sci. Polym. Chem. Ed.* **1981**, *19*, 195.
6. Kast, H.; Funke, W. *Makromol. Chem.* **1979**, *180*, 1335.
7. Keskinel, M.; Okay, O. *Polym. Bull.* **1998**, *40*, 491.
8. Scranton, A. B.; Peppas, N. A. *J. Polym. Sci. Part A: Polym. Chem.* **1990**, *28*, 39.
9. Elliott, J. E.; Anseth, J. W.; Bowman, C. N. *Chem. Eng. Sci.* **2001**, *56*, 3173.
10. Lazzari, S.; Pfister, D.; Diederich, V.; Kern, A.; Storti, G. *Ind. Eng. Chem. Res.* **2014**, *53*, 9035.
11. Flory, P. J. Principles of Polymer Chemistry; Cornell University Press: Ithaca, **1953**, Chapter 3.
12. Zhu, S.; Hamielec, A. E. *Macromolecules* **1993**, *26*, 3131.
13. Andrzejewska, E. *Prog. Polym. Sci.* **2001**, *26*, 605.
14. Buback, M.; Huckenstein, B.; Russel, G. *Macromol. Chem. Phys.* **1994**, *195*, 539.
15. Benson, S. W.; North, A. M. *J. Am. Chem. Soc.* **1962**, *84*, 935.
16. Louie, B.; Carratt, G.; Soong, D. *J. Appl. Polym. Sci.* **1985**, *30*, 3985.
17. Stickler, M. *Makromol. Chem.* **1983**, *184*, 2563.
18. Babayevsky, P. G.; Gillham, J. K. *J. Appl. Polym. Sci.* **1973**, *17*, 2067.
19. Rimdusit, S.; Ishida, H. *Rheol. Acta* **2002**, *41*, 1.
20. Tung, C. Y. M.; Dynes, P. J. *J. Appl. Polym. Sci.* **1982**, *27*, 569.
21. Barner-Kowollik, C.; Vana, P.; Davis, T. P. Handbook of Radical Polymerization; Matyjaszewski, K.; Davis, T. P., Eds.; John Wiley and Sons, Inc: Hoboken, **2002**, Chapter 4.
22. Anseth, K. S.; Wang, C. M.; Bowman, C. N. *Macromolecules* **1994**, *27*, 650.
23. Mateo, J. L.; Serrano, J.; Bosch, P. *Macromolecules* **1997**, *30*, 1285.
24. Mateo, J. L.; Calvo, M.; Serrano, J.; Bosch, P. *Macromolecules* **1999**, *32*, 5243.
25. Bastide, J.; Leibler, L. *Macromolecules* **1988**, *21*, 2647.
26. Matsumoto, A.; Matsuo, H.; Ando, H.; Oiwa, M. *Eur. Polym. J.* **1989**, *25*, 237.
27. Baselga, J.; Llorente, M.; Hernandez-Ruentes, I.; Pierola, I. *Eur. Polym. J.* **1989**, *25*, 471.
28. Peak, C. W.; Wilker, J. J.; Schmidt, G. *Colloid Polym. Sci.* **2013**, *291*, 2031.

29. Kim, B.; Hong, D.; Chang, W. V. *J. Appl. Polym. Sci.* **2013**, *130*, 3574.
30. Kim, B.; Hong, D.; Chang, W. V. *RSC Adv.* **2014**, *4*, 63559.
31. Ward, J. H.; Peppas, N. A. *Macromolecules* **2000**, *33*, 5137.
32. Allcock, H. R.; Lampe, F. W. Contemporary Polymer Chemistry, 2nd ed; Prentice-Hall: New Jersey, **1990**, Chapter 13.
33. Batch, G. L.; Macosko, C. W. *J. Appl. Polym. Sci.* **1992**, *44*, 1711.
34. Kim, B.; Hong, D.; Chang, W. V. *J. Appl. Polym. Sci.* **2014**, *131*, 41026.
35. Carothers, W. H. *Chem. Rev.* **1931**, *8*, 353.
36. Flory, P. J. *J. Am. Chem. Soc.* **1941**, *63*, 3083.
37. Malkin, A. Y.; Kulichikhin, S. G.; Emel'yanov, D. N.; Smetanina, I. E.; Ryabokon, N. V. *Polymer* **1984**, *25*, 778.
38. Zlatanic, A.; Lava, C.; Zhang, W.; Petrovic, Z. S. *J. Polym. Sci. Part B: Polym. Phys.* **2004**, *42*, 809.
39. Flory, P. J. *Ind. Eng. Chem.* **1946**, *38*, 417.
40. Mullins, L.; Thomas, A. G. *J. Polym. Sci.* **1960**, *43*, 13.
41. Tobolsky, A. V.; Metz, D. J.; Mesrobian, R. B. *J. Am. Chem. Soc.* **1950**, *72*, 1942.
42. Tobita, H.; Hamielec, A. E. *Polymer* **1990**, *31*, 1546.
43. Okay, O.; Bahmtas, N. K.; Naghash, H. J. *Polym. Bull.* **1997**, *39*, 233.
44. Okay, O.; Naghash, K.; Capek, I. *Polymer* **1995**, *36*, 2413.
45. Naghash, H. J.; Okay, O. *J. Appl. Polym. Sci.* **1996**, *60*, 971.
46. Lattuada, M.; Gado, E. D.; Abete, T.; de Arcangelis, L.; Lazzari, S.; Diederich, V.; Storti, G.; Morbidelli, M. *Macromolecules* **2013**, *46*, 5831.
47. Beuermann, S.; Buback, M. *Prog. Polym. Sci.* **2002**, *27*, 191.
48. Buback, M.; Feldermann, A.; Barner-Kowollik, C.; Lacik, I. *Macromolecules* **2001**, *34*, 5439.
49. Ballard, M. J.; Napper, D. H.; Gilbert, R. G. *J. Polym. Sci. Part A: Polym. Chem.* **1986**, *24*, 1027.
50. Garrett, R. W.; Hill, D. J. T.; O'Donnell, J. H.; Pomery, P. J.; Winzor, C. L. *Polym. Bull.* **1989**, *22*, 611.
51. Ovando-Medina, V. M.; Corona-Rivera, M. A.; Márquez-Herrera, A.; Lara-Ceniceros, T. E.; Manríquez-González, R.; Peralta, R. D. *J. Appl. Polym. Sci.* **2014**, *131*, 40191.
52. Kienle, R. H.; van der Meulen, P. A.; Petke, F. E. *J. Am. Chem. Soc.* **1939**, *61*, 2258.
53. Bradley, T. F. *Ind. Eng. Chem.* **1938**, *30*, 689.
54. Turnbull, D.; Fisher, J. C. *J. Chem. Phys.* **1949**, *17*, 71.
55. Avrami, M. *J. Chem. Phys.* **1939**, *7*, 1103.
56. Avrami, M. *J. Chem. Phys.* **1940**, *8*, 212.
57. Jena, A. K.; Chaturvedi, M. C. Phase Transformation in Materials; Prentice Hall: New Jersey, **1992**, Chapter 7.
58. Johnson, W. A.; Mehl, K. F. *Trans. AIME* **1939**, *135*, 416.
59. Kloosterboer, J. G. *Adv. Polym. Sci.* **1988**, *84*, 1.